

# Equilibrium and dynamical properties of the ANNNI chain at the multiphase point

Abhishek Dhar, B. Sriram Shastry and Chandan Dasgupta  
*Physics Department, Indian Institute of Science, Bangalore 560012, India.*  
 (February 1, 2008)

We study the equilibrium and dynamical properties of the ANNNI (axial next-nearest-neighbor Ising) chain at the multiphase point. An interesting property of the system is the macroscopic degeneracy of the ground state leading to finite zero-temperature entropy. In our equilibrium study we consider the effect of softening the spins. We show that the degeneracy of the ground state is lifted and there is a qualitative change in the low temperature behaviour of the system with a well defined low temperature peak of the specific heat that carries the thermodynamic “weight” of the ground state entropy. In our study of the dynamical properties, the stochastic Kawasaki dynamics is considered. The Fokker-Planck operator for the process corresponds to a quantum spin Hamiltonian similar to the Heisenberg ferromagnet but with constraints on allowed states. This leads to a number of differences in its properties which are obtained through exact numerical diagonalization, simulations and by obtaining various analytic bounds.

PACS numbers: 05.50.+q, 02.50.Ey, 05.40.-a

## I. INTRODUCTION

The ANNNI chain is one of the simplest systems with competing interactions. It is defined by the following Ising spin Hamiltonian:

$$H = \sum_{i=1}^L (J_1 s_i s_{i+1} + J_2 s_i s_{i+2}), \quad s_i = \pm 1. \quad (1)$$

For  $J_2 > 0$ , the interactions are competing and one can have different ground states depending on the relative strengths of the interactions. A specially interesting case is the point  $J_1 = 2J_2$ , the so-called multiphase point, where the ground state is no longer unique. It can be shown that any spin configuration, which does not have three consecutive spins of the same sign, is a ground state. For a chain of length  $L$ , the number of ground states  $\sim \mu^L$ , where  $\mu = (\sqrt{5} + 1)/2$  is the golden mean. Thus there are an exponentially large number of degenerate ground states and the system has finite zero-temperature entropy per spin. The model has been extensively studied both in one and higher dimensions and is known to have a rich and interesting phase diagram [1]. In this paper we consider some aspects of the equilibrium and dynamical behaviour of the ANNNI chain at the multiphase point.

In our equilibrium study we consider the effect of softening the spins, that is allowing them to take continuous instead of discrete values. It is usual in the study of spin models to consider soft-spin versions of discrete spin models. A well-known example is the Ginzberg-Landau Hamiltonian which is a continuum version of the discrete Ising model. Other examples occur in the study of spin glass models. For instance, the soft spin version of the Sherrington-Kirkpatrick (SK) [2] model was studied [3] in the context of dynamics. The reason for going to soft-spin versions is that they are often more amenable to

theoretical approaches. It is usually expected that qualitatively the soft and hard spin versions should show similar behaviour.

For models with multiple ground states, arising out of frustration, softness may however change the degeneracy completely, as may be seen in a three-spin example, or as in the present case as we shall show here. The effect of spin-softening in systems with competing interactions has been studied earlier by several authors. Seno and Yeomans [4] have looked at the effect of softening spins at the multiphase point of a clock-model. They find, using a perturbative method, that as a softness parameter is varied the system goes through a series of different ground states. In this work we use a similar perturbative method to prove that the macroscopic degeneracy of the ground state in the ANNNI model is lifted by the smallest amount of softness. We then show explicitly how the release of the zero-temperature entropy results in qualitative differences in the low temperature properties of the system. This is similar to the recently observed phenomena of entropy release in spin-ice systems [5]. We also construct an effective hard-spin Hamiltonian to describe the low-temperature properties of the soft-spin model. We have also performed Monte Carlo simulations on the soft-spin model and verified the low-temperature predictions of the effective Hamiltonian.

In the second part of the paper we look at the dynamical properties of the system. As noted before, the ANNNI model at the multiphase point has a large number of degenerate ground states. It is, therefore, of interest to look at dynamical properties of the system at low temperatures. Here we use Kawasaki dynamics to evolve the system and consider zero temperature properties only. Thus two nearest neighbor spins flip with a rate  $\gamma$ , provided both magnetization and energy are conserved. This dynamics has been studied earlier by Das and Barma [6]. In this paper we extend their studies by using the correspondence between  $W$ -matrices for stochastic processes and quantum spin chains.

The correspondence between the stochastic Fokker-Planck operator and quantum chains has often been ex-

exploited to derive dynamical properties. For instance, the scaling, with system size, of the first excited state of the quantum Hamiltonian gives the dynamical exponent of the stochastic process. A well-known example where this correspondence has been used is in exclusion processes [7], which are stochastic models of hard-core diffusing particles. For such processes, it has been possible to exactly calculate the dynamic exponent by solving the corresponding quantum model, namely the Heisenberg model [8]. The dynamics considered by us is very similar to the symmetric exclusion process (SEP) but with added restrictions on allowed moves. To see this we first note that with the present dynamics, nearest neighbor spins with opposite signs flip, provided that the resulting configuration satisfies the ground state constraint of no three successive spins having same signs. Identifying up spins with particles and down spins with holes we see that the dynamics is equivalent to hard core particles diffusing on a lattice with the constraint that there cannot be three successive particles or holes. An interesting question is whether these rather strong constraints make the system different from the SEP. Earlier numerical work [6] seems to suggest that the dynamics still behaves like the SEP. We note that there have been some other recent studies on exclusion processes with constraints on allowed configurations [9]. These cases are solvable by the Bethe ansatz and show the same behaviour as the unconstrained model.

Here we address this question of the effect of the constraints by studying the quantum Hamiltonian. By means of exact numerical diagonalization for finite chains and through analytic bounds, we have tried to understand the differences and similarities of the present Hamiltonian with the Heisenberg Hamiltonian for the SEP. We also discuss the different symmetry properties of the two quantum models. The Heisenberg model has full rotational symmetry and this has several important implications some of which are of direct relevance in understanding the original stochastic process. For example it implies that two-point time correlations in the SEP do not depend on the number of particles. The present model, on the other hand is only invariant under rotations in the  $XY$  plane.

The rest of the paper is divided into two sections. In section (II), we consider equilibrium properties of the soft-spin model while in section (III) we consider the dynamics of the hard-spin model. Section (IV) contains a summary of our main results and a few concluding remarks.

## II. SOFT-SPIN ANNNI MODEL

We consider the following soft spin version of the ANNNI model:

$$H_s = \sum_i J(2s_i s_{i+1} + s_i s_{i+2}) + a g(s_i^4/4 - s_i^2/2),$$

$$s_i \in (-\infty, \infty) \quad (2)$$

where  $a$  is a dimensionless parameter which controls the amount of softness. In the limit  $a \rightarrow \infty$  we get the hard-spin model. We will set  $g = 1$  since there is no loss of generality in doing so.

Let us first look at the ground states of the soft-spin Hamiltonian given by Eqn. (2). To do so we look at the extrema of  $H_s$  which are obtained by setting  $\partial H/\partial s_i = 0$  for all  $i$ . This gives:

$$2J(s_{i+1} + s_{i-1}) + J(s_{i+2} + s_{i-2}) + a(s_i^3 - s_i) = 0 \quad (3)$$

Solving this set of coupled nonlinear equations in general is very difficult. However for small values of the parameter  $1/a$  we can obtain the solutions perturbatively. For  $a \rightarrow \infty$  all configurations,  $\{s_i\}$ , with  $s_i = 0, \pm 1$  are solutions. Those with  $\{s_i = \pm 1\}$  correspond to the minima. For finite but large  $a$  we try to obtain the solutions perturbatively with  $1/a$  acting as the perturbation parameter. We denote the unperturbed minima by the set  $\{t_i = \pm 1\}$ . Let us try the following perturbative expansion:

$$s_i = \sum_{n=0}^{\infty} t_i^{(n)} \left(\frac{1}{a}\right)^n, \quad (4)$$

where the coefficients  $t_i^{(n)}$  are independent of  $a$  and  $t_i^{(0)} \equiv t_i = \pm 1$  correspond to the unperturbed solutions in the limit  $a \rightarrow \infty$ . Plugging this into Eqn. (3), we get

$$J[2(t_{i+1} + t_{i-1}) + (t_{i+2} + t_{i-2})] + \frac{J}{a}[2(t_{i+1}^{(1)} + t_{i-1}^{(1)}) + (t_{i+2}^{(1)} + t_{i-2}^{(1)})] + 2t_i^{(1)} + \frac{1}{a}(3t_i(t_i^{(1)})^2 + 2t_i^{(2)}) + O\left(\frac{1}{a^2}\right) = 0.$$

Equating different powers of  $1/a$  to zero we then get:

$$t_i^{(1)} = \frac{-J}{2}[2(t_{i+1} + t_{i-1}) + (t_{i+2} + t_{i-2})] + O\left(\frac{1}{a}\right)$$

$$t_i^{(2)} = \frac{-J}{2}[2(t_{i+1}^{(1)} + t_{i-1}^{(1)}) + (t_{i+2}^{(1)} + t_{i-2}^{(1)})] - \frac{3}{2}t_i(t_i^{(1)})^2$$

and so on. Thus we get  $2^L$  perturbed minima given by the above perturbation series. The energies corresponding to these minima can now be found by putting these solutions into the expression for energy in Eqn. (2). We thus get

$$E = E_0 + E_1 + E_2 + O(1/a^2), \quad \text{where}$$

$$E_0 = \frac{-La}{4}$$

$$E_1 = \sum_i J(2t_i t_{i+1} + t_i t_{i+2})$$

$$E_2 = \frac{1}{a} \sum_i [(t_i^{(1)})^2 + 2J(t_i t_{i+1}^{(1)} + t_{i+1} t_i^{(1)}) + J(t_i t_{i+2}^{(1)} + t_{i+2} t_i^{(1)})]$$

$$= \frac{-J^2}{2a} \sum_i (5 + 4t_i t_{i+1} + 4t_i t_{i+2} + 4t_i t_{i+3} + t_i t_{i+4}). \quad (5)$$

In the above expansion,  $E_0$  corresponds to the unperturbed energy, while  $E_1$  and  $E_2$  represent the corrections resulting from the perturbation. In the  $a \rightarrow \infty$  limit the term  $E_1$  causes the energy levels of the  $2^L$  minima to split, with separation between them  $\sim O(J)$ . We recognize  $E_1$  as the Hamiltonian for the hard-spin ANNNI model. Thus the lowest energy level is still  $\mu^L$ -fold degenerate. The term  $E_2$  then causes a further splitting of the ground states into levels with separation  $\sim O(J^2/a)$ .

To see whether or not the macroscopic degeneracy of the ground state survives, we need to consider the interaction Hamiltonian corresponding to the energy term  $E_2$ . Since we are interested in the splitting of the lowest energy level of  $E_1$ , we only consider the restricted subspace of spin configurations which are ground states of  $E_1$ . In this subspace the Hamiltonian corresponding to  $E_2$  can be rewritten as

$$H_2 = \frac{-3LJ^2}{2a} - \frac{J^2}{2a} \sum_i (2t_i t_{i+2} + 4t_i t_{i+3} + t_i t_{i+4}). \quad (6)$$

Thus all the interactions are ferromagnetic. However the ground state of  $H_2$  is not the state with all spins up, since this does not belong to the subspace of ground states of  $E_1$ . To find the ground state, we write the second term in  $H_2$ , which we denote by  $h_2$ , in the following form (the constant factor  $J^2/(2a)$  is suppressed):

$$\begin{aligned} h_2 &= - \sum_i (2t_i t_{i+2} + 4t_i t_{i+3} + t_i t_{i+4}) \\ &= - \sum_{i=(4n+1)} \epsilon(t_i, t_{i+1}, t_{i+2}, t_{i+3} \mid t_{i+4}, t_{i+5}, t_{i+6}, t_{i+7}) \end{aligned}$$

$$\begin{aligned} \text{where } \epsilon(t_1, t_2, t_3, t_4 \mid t_5, t_6, t_7, t_8) &= t_1 t_3 + t_2 t_4 + 2t_3 t_5 \\ &+ 2t_4 t_6 + t_5 t_7 + t_6 t_8 + 2t_1 t_4 + 4t_2 t_5 + 4t_3 t_6 + 4t_4 t_7 + 2t_5 t_8 \\ &+ t_1 t_5 + t_2 t_6 + t_3 t_7 + t_4 t_8 \end{aligned} \quad (7)$$

and the index  $n$  runs from 0 to  $(L/4 - 1)$  (we take  $L$  to be an integral multiple of 4). By enumerating the matrix elements  $\epsilon(t_1, t_2, t_3, t_4 \mid t_5, t_6, t_7, t_8)$  for all allowed spin configurations we find that the lowest energy configuration is obtained for the periodic sequence  $(\uparrow\uparrow\downarrow\uparrow\downarrow\dots)$  and the five other configurations obtained by translating and flipping this. Thus we find that the infinite degeneracy of the ground state is removed and instead we get a six-fold degenerate ground state. We note that the procedure just outlined provides a straight forward method of finding the ground state of any spin Hamiltonian. By numerically solving Eqn. (3) for small lattice sizes ( $L = 12$ ) and finding the minimum energy configurations for  $a$  large enough ( $a = 50$ ), we have verified that the perturbative solutions are quite accurate.

The fact that softening of the spins results in removal of the exponential degeneracy of the ground state means that the finite zero temperature entropy is released and we expect it to show up in the behaviour of the low temperature specific heat. This leads to the soft-spin model having low-temperature properties very different from the hard-spin version as we shall now see.

We note that the hard spin model is easily solvable by transfer-matrix methods and one can exactly compute various thermodynamic properties. In the soft-spin case the transfer-matrix eigenvalue equation becomes an integral equation which we have not been able to solve. Hence we have studied the model by Monte Carlo simulations. We have used a dynamics which allows three kinds of processes;

- (i) single spin-flip moves,
- (ii) moves in which two nearest neighbor spins are simultaneously flipped and
- (iii) moves which change the length of a spin.

All three kinds of processes occur with usual Metropolis rates. The reason for allowing both single and double spin-flips is the following. We find that in the hard-spin case, equilibration times, with a single-spin flip dynamics, become very large at low temperatures. On the other hand, allowing for two-spin flips results in very fast equilibration. This is related to the fact that while the single spin-flip dynamics at  $T = 0$  is non-ergodic, including double-flips makes it ergodic. We expect a similar situation even in the case of soft-spins and so have included both (i) and (ii). Finally (iii) is necessary since the spins are now continuous variables and we need to be able to change their lengths.

In order to compare the properties of the soft-spin model with those of the hard-spin one, it is necessary to subtract from the soft-spin free energy a part corresponding to the continuum degrees of freedom. We thus look at the following free energy:

$$F = (-1/\beta)[\ln \text{Tr} e^{-\beta H_s} + L \ln(2) - \ln \text{Tr} e^{-\beta H_g}], \quad (8)$$

where  $H_s$  is as in Eqn. (2),  $H_g = \sum_i a(s_i^4/4 - s_i^2/2)$ , and  $\text{Tr}$  indicates integration over all spin variables. We note that the above expression for the free energy is equivalent to writing the partition function in the form

$$\begin{aligned} Z &= \text{Tr} e^{-\beta H} P(\bar{s}) \quad \text{with} \\ P(\bar{s}) &= \prod_i \frac{2e^{-\beta a(s_i^4/4 - s_i^2/2)}}{\int ds_i e^{-\beta a(s_i^4/4 - s_i^2/2)}}. \end{aligned} \quad (9)$$

$H$  being the original hard-spin Hamiltonian and  $P(\bar{s})$  a probability distribution over the spin variables. In the limit  $a \rightarrow \infty$  this exactly reduces to the hard-spin partition function while at  $T \rightarrow \infty$  one gets  $Z = 2^L$ . From our simulations we get properties corresponding to the first part of the free energy in Eqn. (8). The second part simply corresponds to a noninteracting system and its properties can be easily computed numerically.

In Fig. 1 we plot the specific heat data  $C(T)$  for both the soft-spin and hard-spin models. The hard-spin result is exact and corresponds to infinite system size while the soft-spin data is from simulations on a chain of length  $L = 24$ . The values of various parameters used in the simulation were  $a = 50$  and  $J = 1$ . The high temperature ( $T > 1$ ) data was obtained by averaging over  $10^6$  Monte Carlo steps while the low temperature data is over  $10^7$

steps. As expected we find a second peak in the specific heat at low temperatures. For the hard-spin case the total area under the curve for  $C(T)/T$  is equal to  $\ln(2/\mu)$ . The ground state entropy,  $\ln(\mu)$ , which is released when the spins are softened, is mostly accounted for by the area under the low temperature peak.

The low temperature properties are quite well reproduced by the effective Hamiltonian,  $H_2$ , which describes the energy levels in the lowest band. The thermodynamic properties of  $H_2$  can be exactly calculated by transfer matrix methods, both for finite system sizes and in the infinite size limit. In Fig. 2 we plot the soft-spin low temperature simulation data  $C(T)$  for two system sizes and compare them with results obtained from the effective Hamiltonian. We see good agreement between the two. We also show the infinite system size  $C(T)$  curve obtained from the Hamiltonian  $H_2$ . It is interesting to note that the peak value of the specific heat first increases with system size and then starts decreasing beyond a certain size.

### III. KAWASAKI DYNAMICS OF THE HARD-SPIN ANNI MODEL AT THE MULTIPHASE POINT

As for the usual exclusion process, the quantum Hamiltonian corresponding to our process can be easily written and is given by:

$$\mathcal{H} = \mathcal{P} \left\{ \sum_{k=1}^L -[(\sigma_k^+ \sigma_{k+1}^- + \sigma_k^- \sigma_{k+1}^+) + \frac{1}{2}(\sigma_k^z \sigma_{k+1}^z - 1)] P_k \right\} \mathcal{P} \quad (10)$$

where  $\sigma_k^\alpha$  are the usual Pauli matrices,  $P_k$  are local projection operators given by

$$P_k = (1 - \sigma_{k-2} \sigma_{k-1})(1 - \sigma_{k+2} \sigma_{k+3})/4 \quad (11)$$

and  $\mathcal{P} = \prod_{k=1}^L P_k$  is a global projection operator which projects onto the space of allowed states, *i.e.* those that satisfy the ground state constraint. The spin-flip rate,  $\gamma$ , has been set to unity. Alternatively we can write the Fokker-Planck operator in the following form:

$$\mathcal{H} = - \sum_{k=1}^L (\theta_k + \theta_k^2) \quad \text{where} \\ \theta_k = \mathcal{P} (\sigma_k^+ \sigma_{k+1}^- + \sigma_k^- \sigma_{k+1}^+) \mathcal{P}. \quad (12)$$

The term  $\sum_k \theta_k^2$  is the diagonal term since it corresponds to flipping an unequal pair twice. It is important to write the diagonal part carefully. For instance if in Eqn. (10), the local projection operators,  $P_k$ , were not present, the off-diagonal elements of  $\mathcal{H}$  would still be correct but the diagonal ones would be wrong.

We now study the properties of this quantum Hamiltonian. Our interests are (a) to compare the symmetry properties and conservation laws of the present Hamiltonian with that of the Heisenberg model and (b) to obtain results on the energy gap and hence the dynamical exponent.

#### A. Symmetry properties and conservation laws of the quantum model

We first observe that the  $z$ -component of the total spin,  $S^z$ , commutes with  $\mathcal{H}$ . This simply implies conservation of spin or number of particles in the stochastic model. Thus we can classify energy states into sectors labelled by number of particles  $n$ . The constraints on allowed configurations means that for a lattice of length  $L$  the number of particles can vary over the range  $[L/3] \leq n \leq L - [L/3]$  where  $[L/3]$  denotes the smallest integer greater than or equal to  $L/3$ . It can be shown that except in the lowest and highest sectors, in every other case the dynamics is ergodic. It then follows from detailed balance that the steady state is one in which all allowed configurations in a given sector occur with equal probability. For the quantum model this means that the ground state in any sector is an equally weighted sum over all states ( For the special case where  $L$  is a multiple of 3, the lowest and highest sectors have 3-fold degenerate ground states ).

The other components of the total angular momentum  $S^x$  and  $S^y$  however do not commute with  $\mathcal{H}$ . Thus the present Hamiltonian has  $U(1)$  symmetry instead of the  $SU(2)$  symmetry of the Heisenberg model. Also even though the ground states are degenerate, with one state in every  $S^z$  sector, there is no analogue of the raising/lowering operator  $S^\pm$ . If there were such an operator then the entire eigenvalue spectrum in the  $n$ -particle sector would be a subset of the  $(n-1)$ -particle sector (for  $n < L/2$ ). By looking at the spectrum for finite sized lattices we have verified that this is not so.

To study the presence of long-range order in the ground-state, we have calculated the two-point static correlation functions  $c_z(r) = \langle \sigma_0^z \sigma_r^z \rangle$  and  $c_\pm(r) = \langle \sigma_0^+ \sigma_r^- \rangle$  in the ground state for the half-filled sector. The simple characterization of the ground states in terms of disallowed subsequences enables calculation of ground-state expectation of any operator by means of transfer matrices. The transfer matrix method sums over all the different particle sectors, but in the thermodynamic limit the half filled sector dominates, and so we get correct results (To compute expectation values in other sectors one would need to introduce a chemical potential). Thus we find that  $c_z(r) = A \cos(\phi - 2\pi r/3) e^{-r/\xi}$  where  $\xi = 1/\log((3 + \sqrt{5})/2) = 1.03904\dots$  and  $A$  and  $\phi$  are constants that have different values on odd and even sites. Fourier transforming  $c(r)$  gives the structure factor  $\langle \sigma^z(-q) \sigma^z(q) \rangle$  which has the form shown in

Fig. 3. We note that it is non-vanishing at all  $q$ . The off-diagonal correlation can similarly be obtained using transfer matrices but the calculation becomes extremely cumbersome. Instead we have computed this correlation numerically for finite lattices and find that it saturates, for large  $r$ , to a constant value, which is given by  $\langle \sigma_- \rangle^2 = 0.02917\dots$  (which has been obtained by using the transfer matrix method).

Thus we find that ground-state correlation functions show the same behaviour as in the Heisenberg chain. For the Heisenberg model  $c_z(r)$  is delta-correlated while  $c_{\pm}(r)$  saturates to the value  $1/4$  (which is much larger than its value in the present model). The presence of off-diagonal long range order means that  $U(1)$  symmetry is broken in the ground state. This is analogous to the breaking of  $SU(2)$  symmetry in the ground state of the Heisenberg model. On the other hand, consider the  $XXZ$  chain [10] defined by the Hamiltonian

$$\mathcal{H} = \sum_{k=1}^L -(\sigma_k^+ \sigma_{k+1}^- + \sigma_k^- \sigma_{k+1}^+) - \frac{\Delta}{2} \sigma_k^z \sigma_{k+1}^z. \quad (13)$$

Away from the two isotropic points ( $\Delta = \pm 1$ ), this has the same symmetry as the present model. It has no long range order in the gapless phase ( $-1 < \Delta < 1$ ) and all correlations  $\langle \sigma^\alpha(0) \sigma^\alpha(r) \rangle$  have power law decays. In the ferromagnetic phase ( $\Delta > 1$ ), the model has a gap and full ferromagnetic long-range order in the ground state, with ultra-local longitudinal correlations namely  $c_z(r) = 1/4$ . Thus we see that as far as ground state correlations are concerned the present model is different from the anisotropic  $XXZ$  chain even though they have the same symmetry properties. Our model is more similar in properties to the ferromagnet ( $\Delta = 1$ ) but has a nontrivial depletion of the condensate, as well as a nontrivial  $\langle \sigma_0^z \sigma_r^z \rangle$  correlation.

Finally we note that rotational invariance of the Heisenberg model means that two-point time correlations are completely determined by single magnon excitations and so have the same behaviour in any  $S_z$  sector [8,11]. This result does not hold in the case of the present model.

A second conserved quantity in the model is the total linear momentum. This follows from the translation invariance of  $\mathcal{H}$ . The momentum operator commutes both with  $\mathcal{H}$  and  $S^z$  so that in each  $S^z$  sector energy states can be labelled by their momentum. Clearly the ground state has zero momentum.

## B. Results on the energy gap

As is well known the first excited state of  $\mathcal{H}$  determines the decay of correlations for the stochastic process. Thus the energy gap  $\Delta \sim 1/L^z$  and this determines the dynamic exponent  $z$ . For the SEP, which corresponds to the Heisenberg ferromagnet, it is known that  $z = 2$ . This simply reflects the diffusive modes in the dynamics.

The dynamics studied here is very similar to the SEP but with the constraints on the allowed number of successive particles and holes. An interesting question is whether these rather strong constraints change the dynamical exponent. Unlike the Heisenberg model where the Bethe ansatz is applicable and yields information on the eigenvalue spectrum, the Hamiltonian in Eqn. (10) is much more complicated and we have not been able to use the Bethe ansatz. We have looked at the eigenvalue spectrum by numerical diagonalization of  $\mathcal{H}$  for small system sizes and also through Monte Carlo simulations. We also obtain various analytic bounds on the energy levels.

### (i) Results of numerical diagonalization of $\mathcal{H}$ and Monte Carlo simulations

We have carried out exact diagonalization of the Hamiltonian in Eqn. (10) for chains of length upto  $L = 22$  at half filling. The diagonalization has been done in the momentum basis. This makes the Hamiltonian block diagonal and enables us to go to quite large chain sizes. We find that for small  $L$  the first excited state occurs at total linear momentum  $q = \pi$  and the gap seems to decrease as  $\sim 1/L$ . However from  $L = 22$  onwards, the first excited state shifts to  $q = 2\pi/L$  and the gap at this momentum decreases as  $\sim 1/L^2$ . In Fig. 4 we show the numerically obtained gaps at the two momenta as a function of system size. We also plot corresponding upper bounds on the gaps (to be derived in the next section).

We note here that though it is usually the first excited state that determines the decay of correlations in the stochastic process, it is possible to construct correlation functions whose decay is governed by some other eigenvalue. As an example consider the operator  $Q = e^{i\frac{\pi}{L} \sum_k k \sigma_k^z}$ . This is the so-called twist operator, first studied by Lieb, Schultz and Mattis [12]. In this case, the decay of the correlation,  $\langle Q(0)Q(t) \rangle$  is determined by the lowest eigenvalue at momentum  $\pi$  since the operator carries momentum  $\pi$ . In Fig. 5 we show the decay constant as determined from the correlation decay for different system sizes and compare them with those obtained from exact diagonalization. The correlation function is obtained from Monte Carlo simulations and can also be used for larger system sizes at which numerical diagonalization becomes too difficult.

### (ii) Exact Bounds

We now find upper bounds on the first excited state. Consider the sector with states which have  $n$  overturned spins. The bounds are obtained by constructing trial wave functions orthogonal to the ground state in each sector. Thus consider the operators  $\sigma^z(q) = \frac{1}{\sqrt{L}} \sum_k \sigma_k^z e^{ikq}$  and the twist operator  $Q$  defined in the previous section. Under translation these operators transform as

$$T\sigma^z(q)T^\dagger = \frac{1}{\sqrt{L}} \sum_k \sigma_{k+1} e^{ikq} = e^{-iq} \sigma^z(q)$$

$$TQT^\dagger = e^{i\frac{\pi}{L}} \sum_k \sigma_{k+1}^z = e^{i2\pi d} Q$$

where  $d = n/L$  is the filling fraction of particles. If  $|0_n\rangle$  is the ground state in the  $n$ -particle sector, then the states  $\sigma^z(q)|0_n\rangle$  and  $Q|0_n\rangle$  have momenta  $q$  and  $2\pi d$  respectively and for  $q \neq 0$  are orthogonal to the ground state, which has zero momentum. Hence the following expectation values give us two different upper bounds on the gap:

$$(a) \quad e_z = \frac{\langle \sigma^z(-q) \mathcal{H} \sigma^z(q) \rangle}{\langle \sigma^z(-q) \sigma^z(q) \rangle} \quad (14)$$

$$(b) \quad e_Q = \langle Q^\dagger \mathcal{H} Q \rangle \quad (15)$$

where  $\langle \dots \rangle$  denotes ground state expectations. We now evaluate (a) and (b). We shall henceforth restrict ourselves to the half-filled sector only, though extensions to other sectors can be done.

(a) To evaluate  $e_z$  we first note that the numerator and denominator in Eqn. (14) can be written in the following equivalent form:

$$\begin{aligned} \langle \sigma^z(-q) \mathcal{H} \sigma^z(q) \rangle &= \frac{1}{2} \sum_l e^{iql} \langle [\sigma_1^z, [\mathcal{H}, \sigma_{l+1}^z]] \rangle \\ \langle \sigma^z(-q) \sigma^z(q) \rangle &= \sum_l e^{iql} \langle \sigma_1^z \sigma_{l+1}^z \rangle \end{aligned} \quad (16)$$

The commutator occurring in the above equation can be evaluated and gives:

$$\begin{aligned} [\sigma_1^z, [\mathcal{H}, \sigma_{l+1}^z]] &= -4\mathcal{P}[(\sigma_1^+ \sigma_2^- + \sigma_1^- \sigma_2^+) p_1(-\delta_{l,L} + \delta_{l,1}) + \\ &4(\sigma_L^+ \sigma_1^- + \sigma_L^- \sigma_1^+) p_L(\delta_{l,L-1} - \delta_{l,L})] \mathcal{P}^\dagger \end{aligned} \quad (17)$$

Inserting this in Eqn. (16), and using translational invariance of the ground state we finally obtain:

$$\begin{aligned} \langle \sigma^z(-q) \mathcal{H} \sigma^z(q) \rangle &= 4[1 - \cos(q)] \langle \mathcal{P} P_1(\sigma_1^+ \sigma_2^- + \sigma_1^- \sigma_2^+) \mathcal{P}^\dagger \rangle \\ &= 2[1 - \cos(q)] \langle \mathcal{P} P_1(1 - \sigma_1^z \sigma_2^z) \mathcal{P} \rangle \end{aligned} \quad (18)$$

where the last step has been obtained using the fact that  $\langle 0|\mathcal{H}|0\rangle = 0$ . As noted before ground-state expectations of any operator can be computed using transfer matrices. The expectation value on the rhs of Eqn. (18) is thus found to have the limiting value (as  $L \rightarrow \infty$ )  $\langle \mathcal{P} P_1(1 - \sigma_1^z \sigma_2^z) \mathcal{P} \rangle = 8 - 16/\sqrt{5}$ . The Fourier transform of  $c_z(r)$ , which gives the structure factor  $\langle \sigma^z(-q) \sigma^z(q) \rangle$ , has already been obtained and was plotted in Fig. 3. We note that it is non-vanishing at all  $q$ . Finally, from Eqns. (14,16) we get  $e_z$  which is plotted in Fig. 6 along with the exact results from finite size diagonalization. Putting  $q = 2\pi/L$  and putting in all numerical factors, we get the following result:

$$\Delta \leq 19.78 \frac{\pi^2}{L^2} \quad (19)$$

(b) We now obtain the other bound using the twist operator,  $Q$ . We first note the following properties of  $Q$ :

$$\begin{aligned} Q^\dagger \sigma_l^+ \sigma_{l+1}^- Q |\{\sigma\}\rangle &= e^{i\frac{2\pi}{L}} \sigma_l^+ \sigma_{l+1}^- |\{\sigma\}\rangle \\ Q^\dagger \sigma_l^- \sigma_{l+1}^+ Q |\{\sigma\}\rangle &= e^{-i\frac{2\pi}{L}} \sigma_l^- \sigma_{l+1}^+ |\{\sigma\}\rangle. \end{aligned} \quad (20)$$

Using these relations we obtain

$$\begin{aligned} \langle 0|Q^\dagger \mathcal{H} Q|0\rangle &= - \sum_k \langle 0|Q^\dagger \mathcal{P}(\sigma_k^+ \sigma_{k+1}^- + \sigma_k^- \sigma_{k+1}^+) P_k \mathcal{P} Q|0\rangle \\ &= - \sum_k \frac{1}{2} \langle 0|Q^\dagger \mathcal{P}(\sigma_k^z \sigma_{k+1}^z - 1) P_k \mathcal{P} Q|0\rangle \\ &= - \cos(2\pi/L) \sum_k \langle 0|\mathcal{P}(\sigma_k^+ \sigma_{k+1}^- + \sigma_k^- \sigma_{k+1}^+) P_k \mathcal{P}|0\rangle \\ &= - \sum_k \frac{1}{2} \langle 0|\mathcal{P}(\sigma_k^z \sigma_{k+1}^z - 1) P_k \mathcal{P}|0\rangle \\ &= \frac{L}{2} [1 - \cos(2\pi/L)] \langle 0|\mathcal{P}(1 - \sigma_k^z \sigma_{k+1}^z) P_k \mathcal{P}|0\rangle, \end{aligned} \quad (21)$$

where in the last step we have again used  $\langle 0|\mathcal{H}|0\rangle = 0$  and translational invariance of the ground state. The expectation value above has already been obtained so that we get, for large  $L$ , the following bound for the gap at momentum  $q = \pi$ .

$$\Delta \leq 0.845 \frac{\pi^2}{L} \quad (22)$$

In Fig. 4 we have plotted both the bounds and the exact finite size results at  $q = 2\pi/L$  and  $q = \pi$  as functions of the system size.

#### IV. SUMMARY

In summary we have studied a one-dimensional spin model with competing interactions and studied its low-temperature equilibrium and dynamical properties. In the equilibrium case we have shown that low temperature properties of the soft-spin and hard-spin versions of the model can be very different. The hard-spin version of the model has an infinitely degenerate ground-state. Through a perturbative calculation we have shown, that as soon as we introduce the slightest amount of softness, the degeneracy is lifted. The ground state energy levels split to form a band which is separated from higher levels by  $\Delta E = O(J)$ . The energy levels within this lowest band are described by an effective hard-spin Hamiltonian, containing ferromagnetic interactions upto fourth neighbour terms. This can be used to approximately derive the low temperature properties of the model. We find reasonably good agreement with results from Monte Carlo simulations of the soft-spin model.

Our results indicate that the fixed-length ( $a \rightarrow \infty$ ) limit is a singular one in our model at low temperatures.

Since the ground state of the soft-spin model for large but finite  $a$  is only six-fold degenerate, it would order into one of these six states as  $T \rightarrow 0$ . This implies the occurrence of a zero-temperature phase transition and the existence of an appropriately defined correlation length that diverges as  $T$  goes to zero. In the fixed-length ( $a \rightarrow \infty$ ) limit, on the other hand, averaging over all the degenerate ground states leads to a finite correlation length even at  $T = 0$ . These results suggest that it would be interesting to study the effects of softening the spins on the thermodynamic behavior of two- and higher-dimensional hard-spin models with extensive ground-state entropy. A well-known model of this kind is the nearest-neighbor Ising antiferromagnet on a triangular lattice [13]. This model does not exhibit any phase transition at a non-zero temperature. The degeneracy-lifting effect of introducing magnitude fluctuations found in our study suggests that soft-spin versions of this and other similar models may exhibit finite-temperature phase transitions. Further investigation of this question would be very interesting.

We believe that the removal of the exponential ground-state degeneracy by the introduction of spin-softness in the model studied here is a special case of a more general phenomenon in which the presence of additional degrees of freedom allows the system to relieve frustration and thus reduce the number of degenerate ground states. Coupling the hard spins to other degrees of freedom, such as elastic variables describing possible deformations of the underlying lattice, would probably have similar effects on the degeneracy of the ground state. It is interesting to note in this context that a “deformable” Ising antiferromagnet on a triangular lattice in which the Ising spins are coupled to elastic degrees of freedom exhibits [14] a Peierls-type phase transition at a non-zero temperature. The ordering of the spins at this transition is accompanied by a distortion of the lattice. In general, it is expected that in real, physical systems, such couplings to other degrees of freedom, however weak, would induce some kind of ordering of the spins as the temperature is reduced toward zero, thereby avoiding the unstable situation of having a non-vanishing entropy per spin at  $T = 0$ .

Many disordered spin systems, such as spin glasses [16], exhibit a large number of nearly-degenerate metastable states arising out of frustration. To take an example, the SK model [2] of infinite-range Ising spin glass is known [16] to have an exponentially large number of local minima of the free energy (locally stable solutions of the TAP equations [15]) at sufficiently low temperatures. These local minima of the free energy become local minima of the energy at  $T = 0$ . The presence of a large number (divergent in the thermodynamic limit) of nearly-degenerate metastable states is crucial in the development of the present understanding [16] of the equilibrium and dynamic properties of this system at low temperatures. Our results about the lifting of degeneracy by the introduction of spin-softness raise the following interesting question: would the low-temperature

properties of a soft-spin version of the SK model differ in any significant way from those of the original model? While soft-spin versions of the SK model have been used in studies [3] of the dynamics, questions about how the number and properties of the metastable states of this model change as the spins are made soft have not been addressed in detail. Further investigation of these issues would be most interesting.

Finally it is interesting to note that a similar way of lowering frustration is to make the coupling constants soft while keeping the spins hard. For example, in the case of the Edwards-Anderson Ising spin glass model, two versions have been studied [17]. One is the  $\pm J$  model where the nearest-neighbor coupling constants randomly take the discrete values  $\pm J$  with equal probability. In the other case, the  $J$ s are chosen from a gaussian distribution. In  $d = 2$ , both these cases are believed to have zero-temperature phase transitions, but the nature of the transition is different in the two cases. This difference again arises because of the different ground-state degeneracies in the two cases. In the  $\pm J$  model, the ground-state is exponentially degenerate, while it is unique (modulo a global inversion of all the spins) in the gaussian case. However in higher dimensions where the transition temperature is finite, critical properties near the transition appear to be the same in both cases.

In our nonequilibrium studies we considered the Kawasaki dynamics and studied the quantum Hamiltonian corresponding to the Fokker-Planck operator for the stochastic process. The spectrum of the Hamiltonian is obtained by numerical diagonalization of finite chains. An interesting crossover of the first excited state from momentum  $\pi$  to  $2\pi/L$  is observed with increase in system size. We have found analytic upper bounds on the gaps at these two momenta. These, along with our numerical diagonalization results suggest that the gap vanishes as  $\sim 1/L^2$  and so the dynamics is diffusive as in SEP. We have also compared the symmetry properties of our Hamiltonian with the Heisenberg model. We find that while the model has the symmetry of the  $XXZ$  model, its ground-state properties are closer to those of the ferromagnetic isotropic point. In summary we have shown that our model is a very nontrivial cousin of the Heisenberg ferromagnet. The exclusion of three adjacent like spins essentially changes the model dynamics, and results in a nontrivially depleted condensate in  $\langle \sigma_0^x \sigma_r^x \rangle$  and a nontrivially gapped  $\langle \sigma_0^z \sigma_r^z \rangle$  correlation function. The existence of a groundstate in every  $S^z$  sector is quite obvious from the stochastic point of view but a nontrivial one within the framework of the quantum system (e.g. the absence of a  $\sigma^-$  operator), and require a deeper understanding.

## V. ACKNOWLEDGEMENTS

We thank Mustansir Barma, Dibyendu Das and Deepak Dhar for useful discussions. AD is grateful to the Poornaprajna Institute for financial support.

- 
- [1] J. M. Yeomans, *Solid State Physics* **41**, 151 (1988).
  - [2] D. Sherrington and S. Kirkpatrick, *Phys. Rev. Lett.* **35**, 1972 (1975).
  - [3] H. Sompolinsky and A. Zippelius, *Phys. Rev B* **25**, 6860 (1982).
  - [4] F. Seno and J. M. Yeomans, *Phys. Rev. B* **50**, 10385 (1994).
  - [5] A. P. Ramirez, A. Hayashi, R. J. Cava, R. Siddharthan, B. S. Shastry, *Nature* 399, 333 (1999).
  - [6] D. Das and M. Barma, *Phys. Rev. E* **60**, 2577 (1999).
  - [7] T. Liggett, *Interacting Particle Systems*, New York, Springer (1985).
  - [8] L. H. Gwa and H. Spohn, *Phys. Rev. A* **46**, 844 (1992).
  - [9] F. C. Alcaraz and R. Z. Bariev, *Phys. Rev. E* **60**, 79 (1999).
  - [10] C. N. Yang and C. P. Yang, *Phys. Rev.* **147**, 303 (1966).
  - [11] M. D. Grynberg and R. B. Stinchcombe, *cond-mat/9908051/*.
  - [12] E. Lieb, T. Schultz and D. Mattis, *Annals of Phys.* **16**, 407 (1961).
  - [13] G. H. Wannier, *Phys Rev.* **79**, 357 (1950); R. M. F. Houtappel, *Physica* **16**, 425 (1950).
  - [14] Z. Y. Chen and M. Kardar, *J. Phys. C* **19**, 6825 (1986); Lei Gu *et al*, *Phys. Rev. B* **53**, 11985 (1996).
  - [15] D. J. Thouless, P. W. Anderson and R. G. Palmer, *Phil. Mag.* **35**, 593 (1977).
  - [16] M. Mezard, G. Parisi and M. A. Virasoro, *Spin glass theory and beyond* (World Scientific, Singapore, 1987).
  - [17] K. Binder and A. P. Young, *Rev. Mod. Phys.* **58**, 801 (1986).

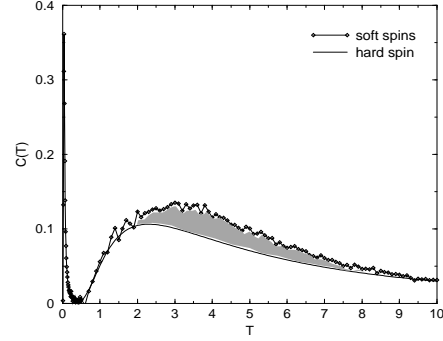


Fig. 1 Dhar, Shastry, Dasgupta

FIG. 1. Simulation data  $C(T)$  for the soft-spin model on a lattice of size  $N = 24$ . A low temperature peak can be seen. For comparison we have also plotted the hard-spin results. Most of the entropy released ( $\sim 85\%$ ) is contained within the low temperature peak while the remaining occurs in the high temperature region (shaded portion).

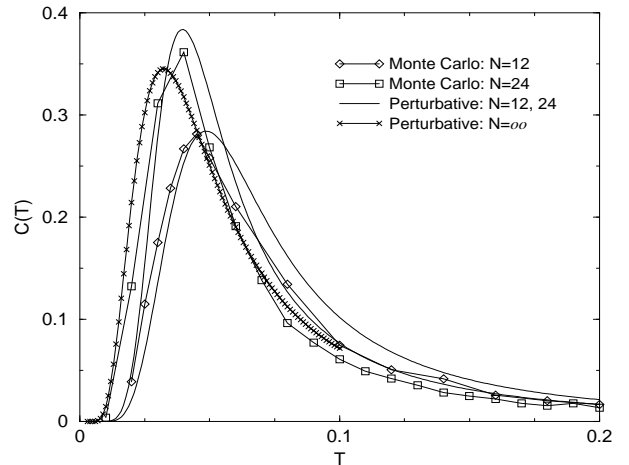


Fig. 2 Dhar, Shastry, Dasgupta

FIG. 2. The plot of  $C(T)$  at low temperatures as obtained from simulations and from the effective Hamiltonian for different system sizes. We also show the effective Hamiltonian result for infinite system size.



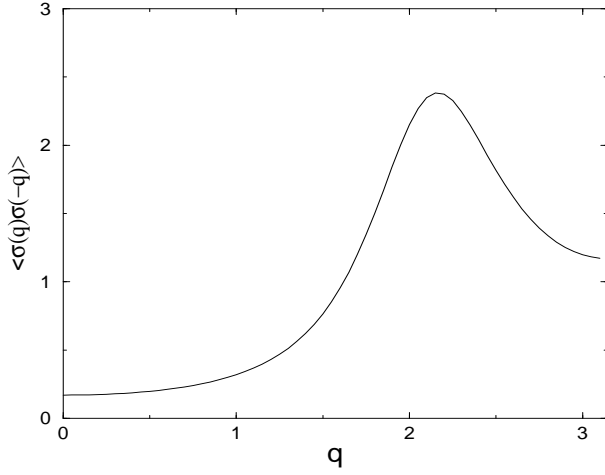


Fig. 3 Dhar, Shastry, Dasgupta

FIG. 3. The diagonal structure factor plotted as a function of the total wave number  $q$ .

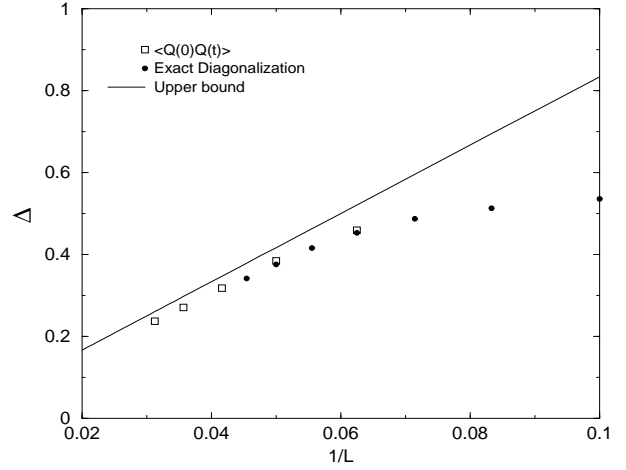


Fig. 5 Dhar, Shastry, Dasgupta

FIG. 5. The energy gap, as obtained from the decay of the correlation function  $\langle Q(0)Q(t) \rangle$  is plotted as a function of inverse system size. Also plotted are the results from exact numerical diagonalization and the upper bound. The diagonalization has been done till system size  $L = 22$  while the  $\langle Q(0)Q(t) \rangle$  data is from Monte Carlo simulations for system size upto  $L = 36$ .

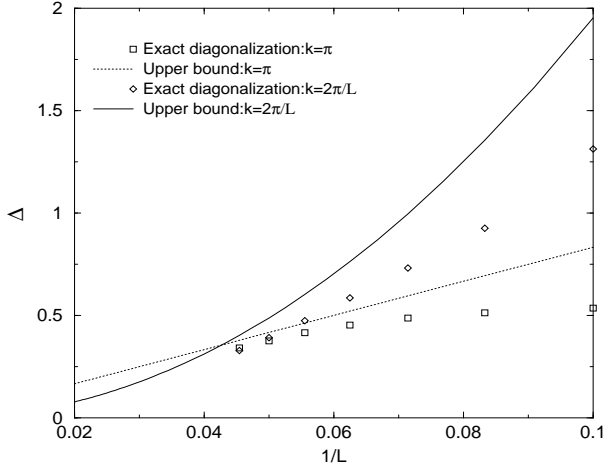


Fig. 4 Dhar, Shastry, Dasgupta

FIG. 4. In this figure the exact energy gaps  $\Delta$  at the two momenta  $\pi$  and  $2\pi/L$  are plotted against inverse system size. Also plotted are exact bounds at the two momenta.

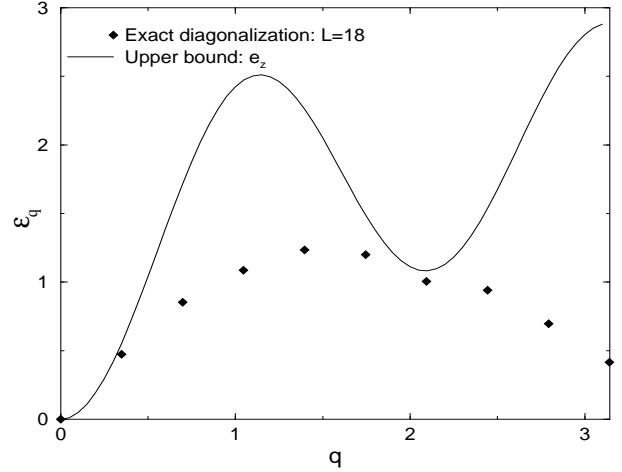


Fig. 6 Dhar, Shastry, Dasgupta

FIG. 6. The gap upper bound,  $e_z$ , plotted as a function of total momentum,  $q$ . The exact eigenvalues for a system of size  $L = 18$  are also shown.